



# Distribution of branched glycerol dialkyl glycerol tetraethers in surface soils of the Qinghai–Tibetan Plateau: implications of brGDGTs-based proxies in cold and dry regions

S. Ding<sup>1</sup>, Y. Xu<sup>1</sup>, Y. Wang<sup>1</sup>, Y. He<sup>2</sup>, J. Hou<sup>2</sup>, L. Chen<sup>3</sup>, and J.-S. He<sup>1,3</sup>

<sup>1</sup>MOE Key Laboratory for Earth Surface Processes, College of Urban and Environmental Sciences, Peking University, Beijing 100871, China

<sup>2</sup>Key Laboratory of Tibetan Environment Changes and Land Surface Processes, Institute of Tibetan Plateau Research, Chinese Academy of Sciences, Beijing 100085, China

<sup>3</sup>Key Laboratory of Adaptation and Evolution of Plateau Biota, Northwest Institute of Plateau Biology, Chinese Academy of Sciences, Xining 810008, China

Correspondence to: Y. Xu (yunpingxu@pku.edu.cn)

Received: 29 October 2014 – Published in Biogeosciences Discuss.: 9 January 2015

Revised: 7 May 2015 – Accepted: 8 May 2015 – Published: 1 June 2015

**Abstract.** The methylation index of branched tetraethers (MBT) and cyclization ratio of branched tetraethers (CBT) based on the distribution of branched glycerol dialkyl glycerol tetraethers (brGDGT) are useful proxies for the reconstruction of mean annual air temperature (MAT) and soil pH. Recently, a series of 6-methyl brGDGTs were identified which were previously co-eluted with 5-methyl brGDGTs. However, little is known about 6-methyl brGDGTs in the Qinghai–Tibetan Plateau (QTP), a critical region of the global climate system. Here, we analyze 30 surface soils covering a large area of the QTP, among which 6-methyl brGDGTs were the most abundant components (average  $53 \pm 17\%$  of total brGDGT). The fractional abundance of 6-methyl brGDGTs showed a good correlation with soil pH, while the global MBT<sub>5ME</sub> calibration overestimates MAT in the QTP. We therefore proposed a MBT<sub>5/6</sub> index including both 5- and 6-methyl brGDGTs, presenting a strong correlation with MAT in QTP:  $\text{MAT} = -20.14 + 39.51 \times \text{MBT}_{5/6}$  ( $n = 27$ ,  $r^2 = 0.82$ ;  $\text{RMSE} = 1.3^\circ\text{C}$ ). Another index, namely IBT (isomerization of branched tetraether), based on carbon skeleton isomerization of the 5-methyl to 6-methyl brGDGTs, is dependent on soil pH:  $\text{pH} = 6.77 - 1.56 \times \text{IBT}$  ( $n = 27$ ;  $r^2 = 0.74$ ,  $\text{RMSE} = 0.32$ ). Our study suggests that changing the position of methyl group of brGDGTs may be another mechanism for some soil

bacteria to adapt to the ambient pH change in addition to the well-known cyclization.

## 1 Introduction

The Qinghai–Tibetan Plateau (QTP), with an area of over 2.5 million km<sup>2</sup> and an average elevation of over 4000 m above sea level (a.s.l.), is the world highest and largest mountain plateau. The uplift of the QTP since the early Cenozoic profoundly influences regional and global climates such as the evolution of the Asian monsoon, which affects the lives of over 2 billion people (An et al., 2001; Li, 1991; Lin et al., 2008; Wang et al., 2008). A number of studies have shown that the QTP is a highly sensitive area for global climate change (e.g., Kang et al., 2010; Liu and Chen, 2000; Qiu, 2008; Yao et al., 2007). The record of 97 meteorological stations located over 2000 m a.s.l. in China reveals that winter temperature rise is of  $0.32^\circ\text{C}$  per decade in the QTP since the 1950s, approximately 3 times the global warming rate (Liu and Chen, 2000). However, the history of instrumental measurements is too short to fully record the evolution of the QTP climate. The reconstruction of the QTP temperature beyond instrumental measurements is challenging because few quantitative proxies are available. Microfossil assemblages based on pollen, diatoms or chironomids are commonly used

paleothermometers but they are also influenced by precipitation, salinity, nutrients or other environmental factors (e.g., Keatley et al., 2009; Meriläinen et al., 2000; Seppä and Birks, 2001). The  $\delta^{18}\text{O}$  value of ice cores in the QTP shows a good correlation with Northern Hemisphere temperature (Thompson et al., 1997; Yao et al., 2002). Unfortunately, ice cores with a long-term, continuous record are lacking in most of the QTP.

Over the past decades, two molecular proxies have been developed for estimation of continental temperature. The first one, namely UK'37, is based on the distribution of haptophyte-derived long-chain alkenones. This proxy was originally proposed for paleoceanography (Brassell et al., 1986; Prahl et al., 1988) but was found applicable for reconstruction of lake surface temperature (e.g., Liu et al., 2006; Zink et al., 2001). A major limitation of UK'37 is that long-chain alkenones are not always present in lakes, although they were reported in some QTP lakes (e.g., Chu et al., 2005; Liu et al., 2006, 2011). In addition, salinity influences the compositions of long-chain alkenones in lakes (Liu et al., 2011). Besides UK'37, the methylation index of branched tetraethers (MBT) and cyclization ratio of branched tetraethers (CBT) can be also used to infer past continental temperature based on the distribution of branched glycerol dialkyl glycerol tetraethers (brGDGT) (Weijers et al., 2007b):

$$\text{MBT} = \frac{\text{Ia} + \text{Ib} + \text{Ic}}{\text{Ia} + \text{Ib} + \text{Ic} + \text{IIa} + \text{IIb} + \text{IIc} + \text{IIIa} + \text{IIIb} + \text{IIIc} + \text{IIa}' + \text{IIb}' + \text{IIc}' + \text{IIIa}' + \text{IIIb}' + \text{IIIc}'}, \quad (1)$$

$$\text{CBT} = -\log \frac{\text{Ib} + \text{IIb} + \text{IIb}'}{\text{Ia} + \text{IIa} + \text{IIa}'}, \quad (2)$$

where roman numbers denote relative abundance of compounds in Fig. 1. It should be pointed out that the Eqs. (1) and (2) are rewritten from original definitions because the peaks previously identified as pure 5-methyl brGDGTs (Weijers et al., 2007b) are actually mixtures of 5-methyl and 6-methyl isomers (De Jonge et al., 2013).

So far, only two species of Acidobacteria were identified to produce brGDGTs (Sinninghe Damsté et al., 2011), but the ubiquitous occurrence of brGDGTs in soils/peats, lakes and marginal seas suggests that other biological sources are likely (Schouten et al., 2013 and references therein). By analyzing globally distributed soils, Weijers et al. (2007b) found that the MBT is controlled by mean annual air temperature (MAT) and to less extent by soil pH, whereas CBT only relates to soil pH. Such relationship was corroborated by the subsequent study of Peterse et al. (2012), who proposed a simplified format of MBT (or MBT') based on seven quantifiable brGDGTs.

Since its advent, the MBT(MBT')–CBT paleotemperature proxy has been increasingly used for lakes (e.g., D'Anjou et al., 2013; Loomis et al., 2012; Sun et al., 2011), paleosol-loess sequences (e.g., Peterse et al., 2011; Zech et al., 2012), peat (Ballantyne et al., 2010) and marginal seas (e.g., Bendle

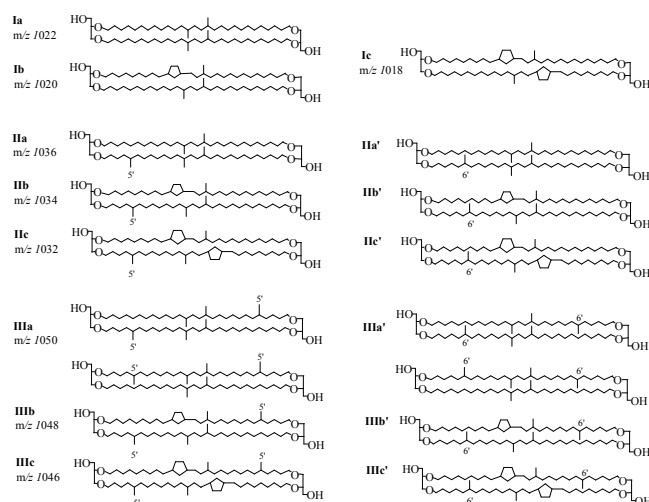


**Figure 1.** Molecular structures of 5- and 6-methyl branched GDGTs used in this study. The compounds that have one or two methyl groups at the  $\alpha 6$  or  $\omega 6$  position are defined as 6-methyl brGDGTs, while the compounds that have one or two methyl groups at the  $\alpha 5$  or  $\omega 5$  position are defined as 5-methyl brGDGTs.

et al., 2010; Weijers et al., 2007a; Zell et al., 2014). However, a relatively large scatter in global MBT/CBT–MAT calibrations (about  $5^\circ\text{C}$  for root mean square error; RMSE) suggests that other factors besides temperature may influence brGDGTs-based indices (Peterse et al., 2012; Weijers et al., 2007b). In arid and semiarid areas such as the western United States, where precipitation is the ecological limiting factor, mean annual precipitation (MAP) rather than MAT is the most important factor that affects brGDGT compositions (Dirghangi et al., 2013; Menges et al., 2014). The updated global calibration of MBT'–CBT indices (Peterse et al., 2012) also shows a weak correlation with MAT for those soil samples from arid regions (MAP < 500 mm). Some studies suggest that regional calibrations are needed to improve accuracy of the GDGTs-based proxy (e.g., Loomis et al., 2012; Pearson et al., 2011; Shanahan et al., 2013; Zink et al., 2010).

Another factor to cause the relatively large scatter of the MBT/CBT–MAT calibration is analytical error. By applying advanced analytical techniques, De Jonge et al. (2013) identified a series of novel 6-methyl brGDGTs which previously co-eluted with 5-methyl GDGTs that were used to calculate the brGDGT proxies. The successful separation of 5- and 6-methyl brGDGTs resulted in a set of new brGDGT proxies, which were used to recalibrate traditionally defined MBT–CBT indexes (De Jonge et al., 2014):

$$\text{MBT}'_{5\text{ME}} = \frac{\text{Ia} + \text{Ib} + \text{Ic}}{\text{Ia} + \text{Ib} + \text{Ic} + \text{IIa} + \text{IIb} + \text{IIc} + \text{IIIa}},$$

$$\text{MAT} = -8.57 + 31.45 \times \text{MBT}'_{5\text{ME}} \quad (3)$$

$$(n = 222, r^2 = 0.66; \text{RMSE} = 4.8^\circ\text{C}, P < 0.001), \quad (4)$$

$$\text{CBT}_{5\text{ME}} = -\log \frac{\text{Ib} + \text{IIb}}{\text{Ia} + \text{IIa}},$$

$$\text{pH} = 7.84 - 1.73 \times \text{CBT}_{5\text{ME}} \quad (5)$$

$$(n = 221, r^2 = 0.60; \text{RMSE} = 0.84, P < 0.001), \quad (6)$$

$$\text{CBT}' = \log \frac{\text{Ic} + \text{IIa}' + \text{IIb}' + \text{IIc}' + \text{IIIa}' + \text{IIIb}' + \text{IIIc}'}{\text{Ia} + \text{IIa} + \text{IIIa}}, \quad (7)$$

$$\text{pH} = 7.15 + 1.59 \times \text{CBT}'$$

$$(n = 221, r^2 = 0.85; \text{RMSE} = 0.52, P < 0.001). \quad (8)$$

For the QTP, several studies have reported GDGTs in lakes, mountains, hot springs and paleosols (e.g., Günther et al., 2014; He et al., 2012; Liu et al., 2013; Wang et al., 2012; Wu et al., 2013; Xie et al., 2012). Wang et al. (2012) analyzed GDGTs in surface sediments of Lake Qinghai and surrounding soils, showing that brGDGTs-inferred MAT and soil pH were consistent with measured values. In contrast, Wu et al. (2013) found that brGDGTs-derived MAT was higher than instrumentally measured MAT in the Kusai Lake sediments from the QTP. Based on the distributions of GDGTs in surface sediments of the QTP lakes, Günther et al. (2014) developed the local calibration of MBT'–CBT' ( $r^2 = 0.59$ ;  $\text{RMSE} = 1.2^\circ\text{C}$ ). However, there are only nine lake sediments included in Günther et al. (2014). For the application of MBT'–CBT' indices in lakes, brGDGTs in lake sediments must be exclusively derived from inputs of surrounding soils. However, in situ production of brGDGTs occurs in various lakes (e.g., Blaga et al., 2009, 2010; Fietz et al., 2012; Pearson et al., 2011; Sinninghe Damsté et al., 2009; Tierney and Russell, 2009). Furthermore, the 6-methyl brGDGTs were not reported in any QTP studies, which may explain the relatively low  $r^2$  value of the MBT'/CBT'–MAT calibration (e.g., Günther et al., 2014). Given these facts, a direct investigation of soils with improved chromatography is needed to understand environmental influences on the brGDGT distributions in the QTP.

Here, we analyzed all 5- and 6-methyl brGDGTs in 30 surface soils from the QTP. Our main objectives are to (1) determine the relative abundance and distribution of 5- and 6-methyl brGDGTs in the QTP soils, (2) evaluate the effect of recently identified 6-methyl brGDGTs on soil pH in the QTP, and (3) test whether global brGDGTs–MAT calibration is applicable in the QTP and thereby understand the influence of temperature, precipitation and soil pH on 5- and 6-methyl brGDGTs in the QTP.

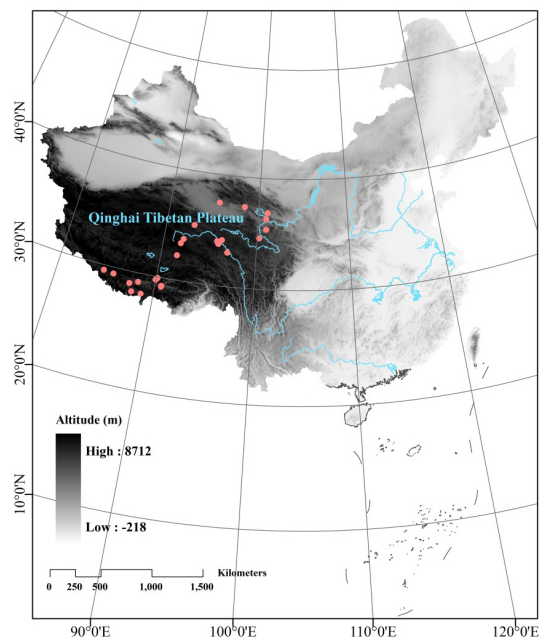


**Figure 2.** Locations of soil sampling sites ( $n = 30$ ) in the QTP (pink solid circles).

## 2 Materials and methods

### 2.1 Sampling

A total of 30 surface soil samples (0–10 cm) were collected during two field works in 2011 and 2012, which cover a large area of the QTP (84.64–101.20° E, 28.24–37.45° N) (Fig. 2). Sampling sites are typical alpine meadow, alpine steppe or alpine meadow steppe. The extremely dry winter results in the lack of persistent snow cover in most sampling sites. The soil samples were air-dried and passed through a 2 mm mesh to remove large gravels. Fine roots (if present) were picked up by steel tweezers. The detailed information on the sampling sites and environmental variables are listed in the Supplement (Table S1).

### 2.2 Climate data

There are about 70 meteorological stations in the QTP, mainly distributed in the eastern part and northern border of the QTP. Thus, direct observation data on temperature and precipitation at our sampling sites are generally lacking. In this study, we use the WorldClim data set (Hijmans et al., 2005) to interpolate annual, seasonal and monthly mean precipitation and temperature (Table S1). The local climate is dry and cold. The MAT of our sampling sites ranges from  $-5.5$  to  $7.6^\circ\text{C}$  with a vertical lapse rate of  $0.487$ – $0.699^\circ\text{C } 100\text{ m}^{-1}$  (Cheng et al., 2012). The vertical lapse rate of air temperature decreases from north to south of the QTP. The MAP at different altitudes varies from ca. 85 to ca. 495 mm. The integrated maps are derived

from monthly temperature and precipitation values gathered from thousands of weather stations around the world from 1950 to 2000 (47 554 locations for precipitation and 24 542 locations for temperature). The original point data were splines interpolated using latitude and longitude at a fine resolution, making it possible to obtain a reasonable estimation of climatic conditions at individual sites. The WorldClim GIS data used contain an annual average of six climate variables at a 30 arcsec resolution ( $\sim 1$  km resolution; <http://www.worldclim.org/current>). Besides MAT and MAP, four additional climate variables were also used to evaluate the relationship between climate and 5- and 6-methyl brGDGT indices, including mean temperature of wettest quarter (MWQT), mean temperature of driest quarter (MDQT), mean temperature of warmest quarter (MWQT'), and mean temperature of coldest quarter (MCQT). A total of 30 sites from QTP cold and dry regions (Table S1) were extracted with six climate variables using Arcgis 9.3.

### 2.3 Soil pH and brGDGT analyses

For pH measurement, soils were mixed with deionized water in a ratio of 1/2.5 ( $\text{g mL}^{-1}$ ). The soil pH values were determined by a pH meter with a precision of  $\pm 0.01$  pH. The pH was reported as an average of three duplicate measurements for each sample with standard deviation of  $\pm 0.05$ .

The detailed procedure for lipid extraction was described by Wu et al. (2014). About 6 g of dry soils was mixed with 600 ng  $\text{C}_{46}$  GDGT (internal standard) (Huguet et al., 2006) and ultrasonically extracted with 20 mL dichloromethane (DCM)/methanol (3 : 1 v : v) for 15 min (3 times). The combined extracts were concentrated to near dryness by a rotary evaporator and transferred to small vials. The concentrated extracts were completely dried under a mild stream of  $\text{N}_2$  and redissolved in DCM. The total extracts were separated into two fractions by 5 mL hexane/DCM (9 : 1 v : v) and 5 mL DCM/methanol (1 : 1 v : v), respectively, on silica gel columns. The latter fraction containing brGDGTs was dissolved in 300  $\mu\text{L}$  hexane/EtOAc (84 : 16 v : v).

The GDGTs were analyzed on an Agilent 1200 high-performance liquid chromatography–atmospheric pressure chemical ionization–triple quadrupole mass spectrometry (HPLC-APCI-MS<sup>2</sup>) system (Yang et al., 2015). The injection volume was 10  $\mu\text{L}$ . The separation of 5- and 6-methyl brGDGTs was achieved with two silica columns in sequence (150 mm  $\times$  2.1 mm; 1.9  $\mu\text{m}$ ; Thermo Finnigan, USA) at a constant flow of 0.2  $\text{mL min}^{-1}$ . The solvent gradient was 84 % A (hexane) and 16 % B (EtOAc) for 5 min, then the amount of B increased from 16 % at 5 min to 18 % at 65 min, and then to 100 % B in 21 min. The column was flushed with 100 % B for 4 min, and then back to 84/16 A/B to equilibrate it for 30 min. The APCI and MS conditions were a vaporizer pressure of  $4.2 \times 10^5$  Pa, vaporizer temperature of 400  $^\circ\text{C}$ , drying gas flow of 6  $\text{L min}^{-1}$ , temperature of 200  $^\circ\text{C}$ , capillary voltage of 3500 V, and corona current of 5  $\mu\text{A}$  (3.2 kV).

Peak integration was carried out using Agilent MassHunter. Samples were quantified based on comparisons of the respective protonated-ion peak areas of each GDGT to the internal standard in selected ion monitoring (SIM) mode. The protonated ions were  $m/z$  1050, 1048, 1046, 1036, 1034, 1032, 1022, 1020, 1018 and 744 ( $\text{C}_{46}$  GDGT). Since we assume same response factors among different brGDGTs and  $\text{C}_{46}$  GDGTs, our study can be only regarded as semi-quantification.

### 2.4 Statistical analyses

In order to assess the relationship of 5- and 6-methyl brGDGT distributions with environmental variables such as temperature, precipitation and soil pH, we performed redundancy analysis (RDA) (van den Wollenberg, 1977); a constrained form of the linear ordination method of principal components analysis (PCA). Species (fractional abundance of 15 brGDGT) were centered and standardized with zero average and unit variance before RDA. The significance of the explanatory variances within a 1 % confidence interval was tested with 999 unrestricted Monte Carlo permutations. Subsequently, a series of partial RDAs (pRDA) were performed to constrain the unique and independent influence of individual environmental parameter alone, as well as compared to all other parameters. All statistical analyses were performed with the CANOCO version 4.5 software (Wageningen UR, USA).

## 3 Results and discussion

### 3.1 BrGDGT abundance in the QTP soils

All soil samples except for P790, P840 and P855 contain detectable amounts of brGDGTs. Consequently, 27 soils were used to calibrate brGDGTs' indices in this study. With the application of two silica LC (liquid chromatographic) columns in tandem, 5-methyl and 6-methyl brGDGT isomers were successfully separated, increasing the number of detectable brGDGT compounds from 9 (Peterse et al., 2012; Weijers et al., 2006) to 15 (Fig. 1). There were three tetramethylated brGDGTs (Ia, Ib and Ic), six pentamethylated brGDGTs (IIa, IIb, IIc, IIa', IIb', IIc') and six hexamethylated brGDGTs (IIIa, IIIb, IIIc, IIIa', IIIb', IIIc'). The mean fractional abundance of 5-methyl brGDGTs ( $f_{5\text{ME}}$ ) and 6-methyl brGDGTs ( $f_{6\text{ME}}$ ) was shown in Fig. 3. The 6-methyl brGDGTs accounted for about 53 % of the total amount of brGDGTs, which were dominated by IIa' and IIIa'. Such composition of brGDGTs is different from that of the global soils (239 soils), where 5-methyl brGDGTs (Ia and IIa) are usually the most abundant isomers and 6-methyl brGDGTs only comprise on average 24 % of the total amounts of brGDGTs (De Jonge et al., 2014), suggesting that the brGDGT-producing bacteria may change their membrane lipids to adapt to environmental conditions. So far, two species of Acidobacte-

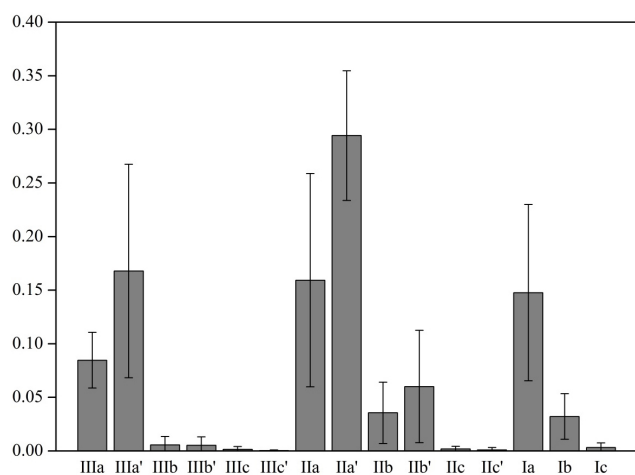


**Figure 3.** Average ( $n = 27$ ) fractional abundance of brGDGTs in surface soils of the QTP.

ria are the only identified biological sources for brGDGTs, but they only produce tetramethylated brGDGTs (Sinninghe Damsté et al., 2011). In our study, the majority of the QTP soils are weak alkaline (6.2–8.4 pH), which may favor the thriving of non-Acidobacteria and thereby lead to the higher proportion of 6-methyl brGDGTs.

### 3.2 Environmental control on brGDGT distributions in QTP

A number of studies have demonstrated that temperature, precipitation and pH are the most important factors that affect the brGDGT distributions in soils (e.g., De Jonge et al., 2014; Dirghangi et al., 2013; Peterse et al., 2012; Weijers et al., 2006, 2007b; Yang et al., 2014, 2015). In order to evaluate the contribution of these parameters to 5- and 6-methyl brGDGT distributions in the QTP, a RDA was performed (Fig. 4). The first component explains 65.2% of the variance, mainly reflecting the variation in soil pH and to less extent MAP. Soil pH presents strong positive relationships with fractional abundance of brGDGTs IIIa', IIb' and IIb, and negative relationships with that of IIIa, IIa and Ia. The second component of the RDA plot explains 6.1% of total variance, mainly reflecting the variation in MAT and MAP. The brGDGTs IIIa', IIIa, IIa, IIb and IIc show negative relationships with MAT (in the lower part of RDA), whereas brGDGTs IIa, Ia, Ib and Ic present positive relationships with MAT (in the upper part of RDA). These results support a physiological mechanism with which soil bacteria change the number of methyl branches of brGDGTs with temperature in order to maintain acceptable fluidity of their membranes (Weijers et al., 2007b).

Our RDA result shows that MAT and pH have a significant independent effect on the brGDGT distribution in the QTP soils; however, no significant correlation was observed between MAP and brGDGTs ( $p > 0.05$ ; Table 1). Soil pH

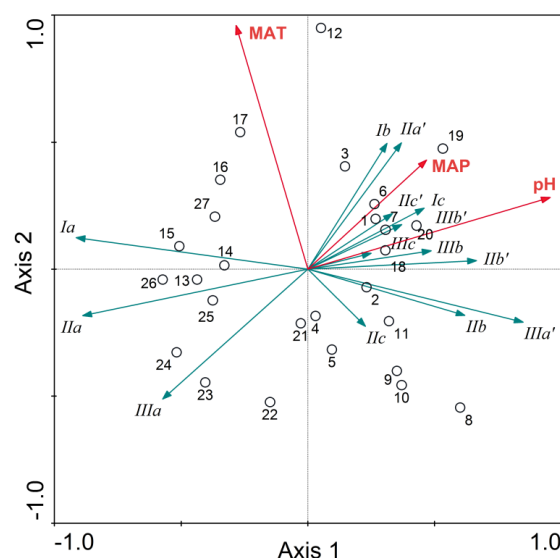


**Figure 4.** RDA triplot showing the relationship between 5- and 6-methyl brGDGT percentages, MAT, MAP and soil pH from the QTP. Numbers in the plot correspond to the soils in the Supplement (Table S1). The first and second axes explained 65.2 and 6.1% of the variance, respectively.

explaining up to 60.1% of the total variables is the largest contributor to the variance, followed by MAT (up to 16.4%) and MAP (up to 10.8%). The predominant influence of soil pH on brGDGT distributions was also observed in the global soil data set (De Jonge et al., 2014; Peterse et al., 2012) and Chinese soils (Yang et al., 2014, 2015). In order to estimate the independent, marginal effect of MAT, MAP and pH, pRDA was performed. The explained variance of pH still remains high (39.9%), indicating that brGDGT distributions are indeed linked to soil pH, whereas MAT contributes to a smaller amount (10.6%) of the variance (Table 1). Similar to the result of RDA, pRDA also showed minor contribution of MAP (2.0%) to brGDGT distributions. The comparison between RDA and pRDA suggests a decreasing contribution of these three environmental variables (pH, MAT, MAP) when they are considered as a unique contribution (Table 1). Thus, there is a “synergistic effect” (an “antagonistic action”) when MAP and pH (MAT and pH) are considered as covariables, resulting in a positive joint effect of 20.4% for the total contributions of pH+MAT+MAP to brGDGT distributions in the QTP soils.

### 3.3 Evaluation of brGDGT-based proxies in the QTP

Since the identification of 6-methyl brGDGTs (De Jonge et al., 2013), a set of new brGDGT indices such as MBT<sub>5ME</sub> and CBT<sub>5ME</sub> have been proposed in order to reduce uncertainty of reconstructed MAT and soil pH (De Jonge et al., 2014; Weijers et al., 2007a; Yang et al., 2015). However, even with application of the MBT<sub>5ME</sub>–MAT recalibration

**Table 1.** Results of RDA and pRDA showing the total and unique contributions of soil pH, MAT and MAP to the variance in brGDGT distributions in the QTP soils.

Variables	Total contribution (%)		Unique contribution (%)	
	<i>p</i> Value	Max eigenvalues*	<i>p</i> Value	Eigenvalues
pH	0.001	60.1	0.001	39.9
MAT	0.001	16.4	0.001	10.6
MAP	0.179	10.8	0.172	2.0
All variables	0.001	72.9		
Joint effects				20.4
MAT + pH	0.001	56.4		
MAT + MAP	0.001	12.8		
MAP + pH	0.001	62.1		

\* The first environmental variable which has been selected into the analysis has the maximum eigenvalues (explained variances), there are six sequences with different arrangements of pH, MAT and MAP. However, no matter which sequence has been selected for RDA, the total variables' contribution is invariant.

and the multiple regression, relatively large scatter still exists for those samples from cold regions (De Jonge et al., 2014). Therefore, further calibrations of brGDGT-derived proxies are needed.

### 3.3.1 MAT calibration in cold and dry regions of the QTP

Consistent with the finding of De Jonge et al. (2014), our result shows that  $CBT_{5ME}$  no longer contributes significantly to MAT after the exclusion of 6-methyl brGDGTs ( $p = 0.51$ ;  $n = 27$ ). Therefore, we use  $MBT'_{5ME}$  only to calibrate MAT. Considering that limited samples from cold regions were included in previous studies (Peterse et al., 2012; Weijers et al., 2007b), we added our QTP data into the global soil data set (De Jonge et al., 2014), resulting in a new calibration of  $MBT'_{5ME}$ -MAT:

$$MAT = -10.07 + 33.50 \times MBT'_{5ME} \quad (9)$$

( $n = 249$ ,  $r^2 = 0.70$ ; RMSE = 4.7 °C,  $P < 0.001$ ).

The correlation coefficient of Eq. (9) ( $r^2 = 0.70$ ) is slightly higher than the previous global calibration ( $r^2 = 0.66$ ; Eq. 4), while its RMSE (4.7 °C) is similar to the previous calibration (4.8 °C; Eq. 4) (De Jonge et al., 2014). Furthermore, the comparison of our estimated MAT and actual MAT ( $\Delta MAT = MAT_{est} - MAT_{act}$ ) showed an apparent overestimation (average 2.8 °C; Fig. 5). Therefore, the simple extension of the data set is not successful in improving accuracy of the  $MBT'_{5ME}$ -MAT proxy at the global scale.

Alternatively, we conducted a regional calibration of  $MBT'_{5ME}$  versus MAT based on 27 QTP soils, and a new equation of  $MBT'_{5ME}$ -MAT was expressed:

$$MAT = -10.82 + 28.36 \times MBT'_{5ME} \quad (10)$$

( $n = 27$ ,  $r^2 = 0.65$ ; RMSE = 1.8 °C,  $P < 0.001$ ).

The slope of Eq. (10) (28.36) is distinctly different from that of the global surface soils (33.50; Eq. 4). Meanwhile, its

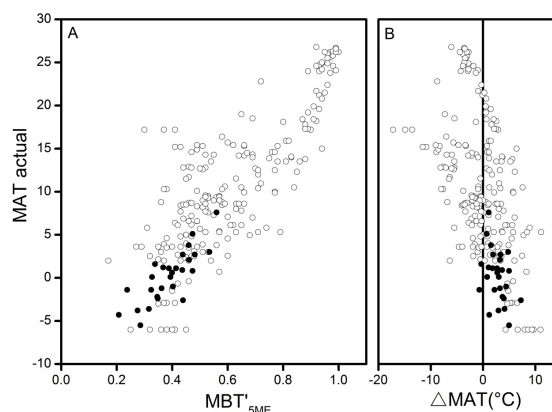


**Figure 5.** (a) Scatterplot of  $MBT'_{5ME}$  with actual MAT; (b) difference between estimated MAT and actual MAT ( $\Delta MAT$ ). Solid and empty circles represented soils in this study and global soils (De Jonge et al., 2014), respectively.

RMSE value (1.8 °C) is substantially smaller than that of De Jonge et al. (2014) (4.8 °C). This reduced uncertainty in reconstructed MAT is attributed to smaller spatial heterogeneity of soils, similar vegetation types (e.g., alpine meadow) and a narrower MAT range (−5.5–7.6 °C) in the QTP. Usually, the regional calibration has higher  $r^2$  values than the global one due to its smaller size of data set and smaller spatial heterogeneity (Loomis et al., 2014; Yang et al., 2014). However, our calibration for the QTP has a slightly lower  $r^2$  value (0.65) than the global one (0.70; Eq. 9), which suggests that the calibration based on  $MBT'_{5ME}$  alone is not superior to the traditional MBT calibration. The RDA result reveals that similar to 5-methyl brGDGTs, 6-methyl brGDGTs also significantly correlate with MAT (Fig. 4). Thus, we propose a new brGDGT index ( $MBT_{5/6}$ ) including 5-methyl brGDGTs used in the traditional definition and two dominant 6-methyl brGDGTs (IIa' and IIIa'), expressed as

$$MBT_{5/6} = \frac{Ia + Ib + Ic + IIa'}{Ia + Ib + Ic + IIa + IIb + IIc + IIIa + IIIa'} \quad (11)$$

Based on data of the QTP soils, the linear correlation of MAT and  $MBT_{5/6}$  was established as (Fig. 7)

$$MAT = -20.14 + 39.51 \times MBT_{5/6}$$

$$(n = 27, r^2 = 0.82; RMSE = 1.3 \text{ °C}, P < 0.001). \quad (12)$$

This calibration has a substantially higher  $r^2$  (i.e., 0.82) and lower RMSE (i.e., 1.3 °C) than Eq. (9) (i.e., 0.70 for  $r^2$  and 4.7 °C for RMSE) and Eq. (10) (i.e., 0.65 for  $r^2$  and 1.8 °C for RMSE), supporting that the inclusion of 5-methyl and 6-methyl brGDGTs is essential for improved accuracy of MAT reconstruction. However, this result is different from the finding at Mount Shennongjia (central China) that 6-methyl brGDGTs are regarded as the interference, leading to a larger scatter of the  $MBT'$ -MAT proxy (Yang et al., 2015).

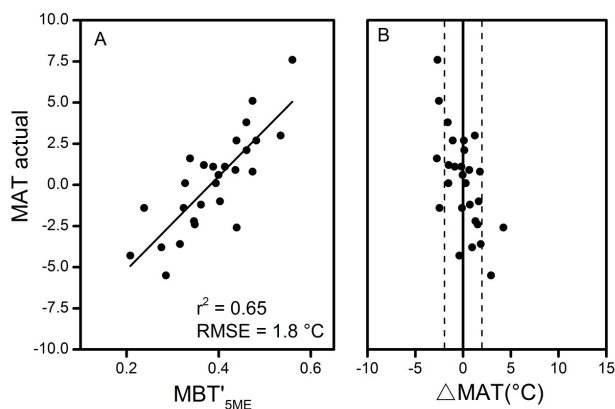


**Figure 6.** (a) Linear regression of  $MBT'_{5ME}$  with actual MAT; (b) difference between estimated MAT and actual MAT ( $\Delta MAT$ ). Data in this study are from 27 surface soils of the QTP.

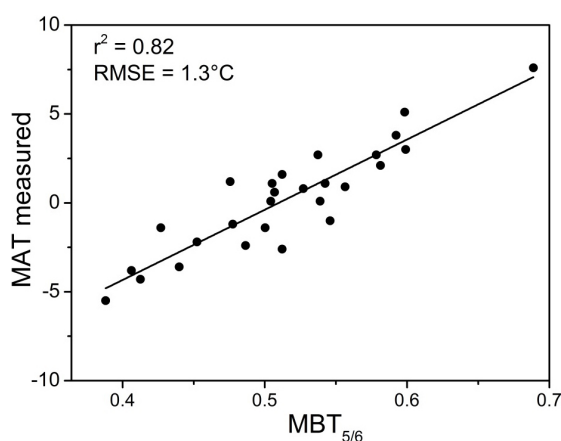


**Figure 7.** Linear regression plot of  $MBT_{5/6}$  versus MAT in the QTP.

Nevertheless, these differences highlight the importance of regional calibrations of brGDGT proxies.

### 3.3.2 Effect of soil pH on position of the methyl group(s) of brGDGTs

It is generally accepted that the proton permeability of the cell membrane plays a crucial role in maintaining the pH gradient across the membrane of bacteria and archaea (Konings et al., 2002). Weijers et al. (2007b) observed a strong correlation between relative abundance of cyclopentane moieties of brGDGTs and soil pH, and hypothesized that some soil bacteria can change the methyl groups of brGDGTs into cyclopentyl groups with ambient pH rise, which will loosen the packing of the membrane lipids, enabling more water molecules to get trapped.

Following the approach of De Jonge et al. (2014), we got the following correlation between soil pH and  $CBT'$  which is a modified format of the originally defined CBT (Weijers

et al., 2007b):

$$\begin{aligned} \text{pH} &= 7.01 + 1.49 \times CBT' \\ n &= 27, r^2 = 0.78, \text{RMSE} = 0.30. \end{aligned} \quad (13)$$

Equation (13) has a slightly lower  $r^2$  and substantially lower RMSE compared with the global calibration of  $\text{pH}-CBT'$  ( $n=221$ ,  $r^2=0.85$ ,  $\text{RMSE}=0.52$ ) (De Jonge et al., 2014), suggesting that both global and regional calibrations are applicable for soil pH reconstruction.

We noted that some non-cyclopentyl brGDGTs such as Ia, IIa and IIIa show negative correlations with soil pH, while other brGDGTs show positive correlations with soil pH in the RDA (Fig. 4). Based on these facts, we put all positively correlated brGDGTs on the numerator and all negatively correlated brGDGTs on the denominator to build a new CBT index (or  $CBT''$ ):

$$CBT'' = \log \frac{Ib + Ic + IIb + IIc + IIIb + IIIc + IIa' + IIb' + IIc' + IIIa' + IIIb' + IIIc'}{Ia + IIa + IIIa}. \quad (14)$$

A linear correlation between soil pH and  $CBT''$  was established based on 27 QTP soils:

$$\begin{aligned} \text{pH} &= 6.93 + 1.49 \times CBT'' \\ (n &= 27, r^2 = 0.80, \text{RMSE} = 0.29). \end{aligned} \quad (15)$$

The similar  $r^2$  and RMSE between Eqs. (13) and (15) was attributed to minor amounts of brGDGTs Ib, IIb, IIc, IIIb and IIIc (average 8 % of total brGDGTs; Fig. 3) which were excluded from the  $CBT'$  index but included in our  $CBT''$  index.

The fractional abundance of 6-methyl brGDGTs showed strong positive correlations with soil pH in both the QTP ( $r^2=0.74$ ; Fig. 8) and global soils data set ( $0.41 < r^2 < 0.72$ ; De Jonge et al., 2014). This is apparent contrast with the previous assumption that non-cyclopentyl moieties (such as IIa' and IIIa') negatively correlate with soil pH. Unlike 6-methyl brGDGTs, some 5-methyl brGDGTs did not show positive correlations with soil pH (De Jonge et al., 2014). Thus, we hypothesize that besides cyclization, the position of methyl group(s) of brGDGTs also influences cell membrane fluidity. In order to test this hypothesis, we define a new index about the carbon skeleton isomerization of branched tetraethers (or IBT) as the abundant ratio of non-cyclopentyl 6-methyl to 5-methyl brGDGTs:

$$IBT = -\log \frac{IIIa' + IIa'}{IIIa + IIa}. \quad (16)$$

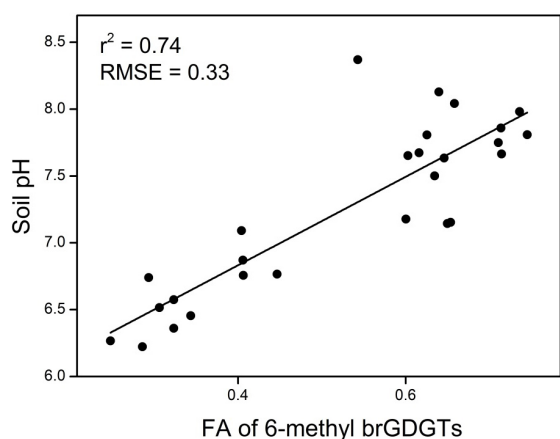


**Figure 8.** Plots of fractional abundance of 6-methyl brGDGTs in the total amount of brGDGTs ( $f_{6ME}$ ) versus soil pH in the QTP.

We performed a linear regression of IBT versus soil pH based on 27 QTP soils (Fig. 9), yielding the equation

$$\text{pH} = 6.77 - 1.56 \times \text{IBT} \quad (n = 27; r^2 = 0.74, \text{RMSE} = 0.32). \quad (17)$$

Meanwhile, the linear correlation of  $\text{CBT}_{5ME}$  and soil pH was also established (Fig. 9):

$$\text{pH} = 7.98 - 1.12 \times \text{CBT}_{5ME} \quad (n = 27; r^2 = 0.66, \text{RMSE} = 0.37). \quad (18)$$

For the regional calibration, the IBT index has a higher  $r^2$  and lower RMSE than the traditionally defined  $\text{CBT}_{5ME}$  index, supporting that the carbon skeleton isomerization of brGDGTs (i.e., changing the position of methyl group) is indeed a physiological mechanism of brGDGTs-producing bacteria to adapt soil pH change.

### 3.3.3 Seasonality of brGDGT proxies in the QTP

The QTP is under strong influence of the Asian Monsoon, characterized by warm/humid summer (June–August) and dry/cold winter (December–February) (An et al., 2001; Qiu, 2008). In order to examine if there is a seasonal bias on brGDGT distributions, we analyze the correlation coefficients of 5- and 6-methyl brGDGT proxies (i.e.,  $\text{MBT}'_{5ME}$ ,  $\text{MBT}_{5/6}$ ,  $\text{CBT}_{5ME}$  and IBT) versus annual and seasonal air temperature (Table S2). Overall, there is no apparent seasonal bias for  $\text{MBT}'_{5ME}$  and  $\text{MBT}_{5/6}$ . This is likely attributed to significant correlation between seasonal temperature and MAT in the QTP ( $r^2 > 0.80$ ,  $p < 0.0001$ ). In addition, no significant correlation was observed between the CBT indices/IBT and MAT/seasonal temperature ( $-0.3 < r < 0.3$ ; Table S2), suggesting minor influence of air temperature on these indices. Our results are consistent with those of Weijers et al. (2011), who found no significant seasonal bias in

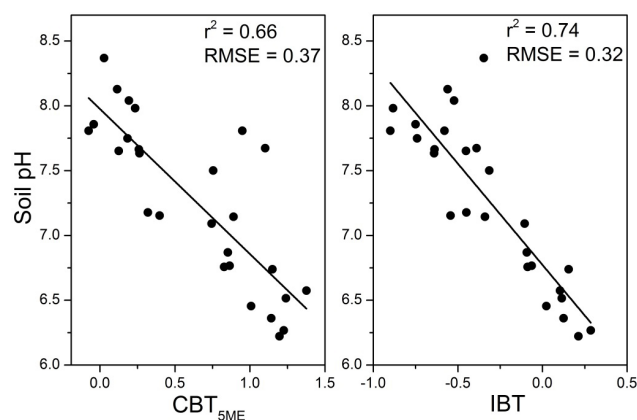


**Figure 9.** Scatterplots of soil pH versus  $\text{CBT}_{5ME}$  and soil pH versus IBT based on 27 soil samples in the QTP.

MBT–CBT indices in mid-latitude soils. Therefore, the reconstruction of MAT based on the 5- and 6-methyl brGDGT proxies is doable in the QTP.

## 4 Conclusions

By applying improved chromatography, we successfully separated 5- and 6-methyl brGDGTs in the surface soils from the QTP, a cold and dry region. This is the first report about 6-methyl brGDGTs in the QTP, providing an opportunity to optimize brGDGTs' proxies in this critical region. Three conclusions were reached based on brGDGT data in 27 surface soils. Firstly, the 6-methyl brGDGTs are widely distributed in the QTP soils, accounting for, on average, 53 % of the total amount of brGDGTs. Secondly, soil pH is the most important contributor to the variance of brGDGTs, followed by MAT, while MAP has no significant effect on brGDGTs' distributions. Thirdly, two new indices including recently identified 6-methyl brGDGTs were proposed to estimate MAT and soil pH, respectively. The first one, namely  $\text{MBT}_{5/6}$ , is useful for the MAT reconstruction in cold and dry regions (like the QTP) with an improved RMSE of 1.3 °C. The second one, namely IBT, allows estimating soil pH with an RMSE of 0.32. Our study demonstrates that besides the previously reported cyclization, isomerization of 5-methyl to 6-methyl brGDGTs (expressed as IBT) is another strategy for brGDGTs-producing bacteria to adapt to the ambient pH change.

**The Supplement related to this article is available online at doi:10.5194/bg-12-3141-2015-supplement.**



**Acknowledgements.** We are grateful to the National Basic Research Program of China (2014CB954001) and the National Science Foundation of China (41176164; 41476062) for financial support. We also thank Huan Yang for assistance in biomarker analyses.

Edited by: Y. Kuzyakov

## References

- An, Z. S., Kutzbach, J. E., Prell, W. L., Porter, and S. C.: Evolution of Asian monsoons and phased uplift of the Himalayan Tibetan plateau since Late Miocene times, *Nature*, 411, 62–66, 2001.
- Ballantyne, A. P., Greenwood, D. R., Sinninghe Damsté, J. S., Csank, A. Z., Eberle, J. J., and Rybczynski, N.: Significantly warmer Arctic surface temperatures during the Pliocene indicated by multiple independent proxies, *Geology*, 38, 603–606, 2010.
- Bendle, J. A., Weijers, J. W. H., Maslin, M. A., Damste, J. S. S., Schouten, S., Hopmans, E. C., Boot, C. S., Pancost, and R. D.: Major changes in glacial and Holocene terrestrial temperatures and sources of organic carbon recorded in the Amazon fan by tetraether lipids, *Geochim. Geophys. Geosy.*, 11, Q12007, doi:10.1029/2010gc003308, 2010.
- Bлага, C. I., Reichart, G.-J., Heiri, O., and Damste, J. S. S.: Tetraether membrane lipid distributions in water-column particulate matter and sediments: a study of 47 European lakes along a north-south transect, *J. Paleolimnol.*, 41, 523–540, 2009.
- Bлага, C. I., Reichart, G.-J., Schouten, S., Lotter, A. F., Werne, J. P., Kosten, S., Mazzeo, N., Lacerot, G., and Sinninghe Damsté, J. S.: Branched glycerol dialkyl glycerol tetraethers in lake sediments: Can they be used as temperature and pH proxies?, *Org. Geochem.*, 41, 1225–1234, 2010.
- Brassell, S. C., Eglinton, G., Marlowe, I. T., Pflaumann, U., and Sarnthein, M.: Molecular stratigraphy: a new tool for climatic assessment, *Nature*, 320, 129–133, 1986.
- Cheng, W., Zhao, S., Zhou, C., and Chen, X.: Simulation of the Decadal Permafrost Distribution on the Qinghai-Tibet Plateau (China) over the Past 50 Years, *Permafrost Periglac.*, 23, 292–300, 2012.
- Chu, G. Q., Sun, Q., Li, S. Q., Zheng, M. P., Jia, X. X., Lu, C. F., Liu, J. Q., and Liu, T. S.: Long-chain alkenone distributions and temperature dependence in lacustrine surface sediments from China, *Geochim. Cosmochim. Ac.*, 69, 4985–5003, 2005.
- D’Anjou, R. M., Wei, J. H., Castañeda, I. S., Brigham-Grette, J., Petsch, S. T., and Finkelstein, D. B.: High-latitude environmental change during MIS 9 and 11: biogeochemical evidence from Lake El’gygytgyn, Far East Russia, *Clim. Past*, 9, 567–581, doi:10.5194/cp-9-567-2013, 2013.
- De Jonge, C., Hopmans, E. C., Stadnitskaia, A., Rijpstra, W. I. C., Hofland, R., Tegelaar, E., and Sinninghe Damsté, J. S.: Identification of novel penta- and hexamethylated branched glycerol dialkyl glycerol tetraethers in peat using HPLC–MS2, GC–MS and GC–SMB–MS, *Org. Geochem.*, 54, 78–82, 2013.
- De Jonge, C., Hopmans, E. C., Zell, C. I., Kim, J.-H., Schouten, S., and Sinninghe Damsté, J. S.: Occurrence and abundance of 6-methyl branched glycerol dialkyl glycerol tetraethers in soils: Implications for palaeoclimate reconstruction, *Geochim. Cosmochim. Ac.*, 141, 97–112, 2014.
- Dirghangi, S. S., Pagani, M., Hren, M. T., and Tipple, B. J.: Distribution of glycerol dialkyl glycerol tetraethers in soils from two environmental transects in the USA, *Org. Geochem.*, 59, 49–60, 2013.
- Fietz, S., Hugué, C., Bendle, J., Escala, M., Gallacher, C., Herfort, L., Jamieson, R., Martinez-Garcia, A., McClymont, E. L., Peck, V. L., Prah, F. G., Rossi, S., Rueda, G., Sanson-Barrera, A., and Rosell-Mele, A.: Co-variation of crenarchaeol and branched GDGTs in globally-distributed marine and freshwater sedimentary archives, *Global Planet. Change*, 92–93, 275–285, 2012.
- Günther, F., Thiele, A., Gleixner, G., Xu, B., Yao, T., and Schouten, S.: Distribution of bacterial and archaeal ether lipids in soils and surface sediments of Tibetan lakes: Implications for GDGT-based proxies in saline high mountain lakes, *Org. Geochem.*, 67, 19–30, 2014.
- He, L., Zhang, C. L., Dong, H., Fang, B., and Wang, G.: Distribution of glycerol dialkyl glycerol tetraethers in Tibetan hot springs, *Geosci. Front.*, 3, 289–300, 2012.
- Hijmans, R. J., Cameron, S. E., Parra, J. L., Jones, P. G., and Jarvis, A.: Very high resolution interpolated climate surfaces for global land areas, *Int. J. Climatol.*, 25, 1965–1978, 2005.
- Hugué, C., Hopmans, E. C., Febo-Ayala, W., Thompson, D. H., Sinninghe Damsté, J. S., and Schouten, S.: An improved method to determine the absolute abundance of glycerol dibiphytanyl glycerol tetraether lipids, *Org. Geochem.*, 37, 1036–1041, 2006.
- Kang, S., Xu, Y., You, Q., Fluegel, W.-A., Pepin, N., and Yao, T.: Review of climate and cryospheric change in the Tibetan Plateau, *Environ. Res. Lett.*, 5, 015101, doi:10.1088/1748-9326/5/1/015101, 2010.
- Keatley, B., Douglas, M. V., Blais, J., Mallory, M., and Smol, J.: Impacts of seabird-derived nutrients on water quality and diatom assemblages from Cape Vera, Devon Island, Canadian High Arctic, *Hydrobiologia*, 621, 191–205, 2009.
- Konings, W., Albers, S.-V., Koning, S., Driessen, and A. M.: The cell membrane plays a crucial role in survival of bacteria and archaea in extreme environments, *Antonie Van Leeuwenhoek*, 81, 61–72, 2002.
- Li, J. J.: The environmental effects of the uplift of the Qinghai-Xizang Plateau, *Quaternary Sci. Rev.*, 10, 479–483, 1991.
- Lin, X., Zhu, L., Wang, Y., Wang, J., Xie, M., Ju, J., Mäusbacher, R., and Schwalb, A.: Environmental changes reflected by n-alkanes of lake core in Nam Co on the Tibetan Plateau since 8.4 kaBP, *Chinese Sci. Bull.*, 53, 3051–3057, 2008.
- Liu, W., Liu, Z., Wang, H., He, Y., Wang, Z., and Xu, L.: Salinity control on long-chain alkenone distributions in lake surface waters and sediments of the northern Qinghai-Tibetan Plateau, China, *Geochim. Cosmochim. Ac.*, 75, 1693–1703, 2011.
- Liu, W., Wang, H., Zhang, C. L., Liu, Z., and He, Y.: Distribution of glycerol dialkyl glycerol tetraether lipids along an altitudinal transect on Mt. Xiangpi, NE Qinghai-Tibetan Plateau, China, *Org. Geochem.*, 57, 76–83, 2013.
- Liu, X. D. and Chen, B. D.: Climatic warming in the Tibetan Plateau during recent decades, *Int. J. Climatol.*, 20, 1729–1742, 2000.
- Liu, Z., Henderson, A. C. G., and Huang, Y.: Alkenone-based reconstruction of late-Holocene surface temperature and salinity changes in Lake Qinghai, China, *Geophys. Res. Lett.*, 33, L09707, doi:10.1029/2006GL026151, 2006.

- Loomis, S. E., Russell, J. M., Ladd, B., Street-Perrott, F. A., and Sinninghe Damsté, J. S.: Calibration and application of the branched GDGT temperature proxy on East African lake sediments, *Earth Planet. Sc. Lett.*, 357–358, 277–288, 2012.
- Loomis, S. E., Russell, J. M., Eggermont, H., Verschuren, D., and Sinninghe Damsté, J. S.: Effects of temperature, pH and nutrient concentration on branched GDGT distributions in East African lakes: Implications for paleoenvironmental reconstruction, *Org. Geochem.*, 66, 25–37, 2014.
- Menges, J., Huguet, C., Alcañiz, J. M., Fietz, S., Sachse, D., and Rosell-Melé, A.: Influence of water availability in the distributions of branched glycerol dialkyl glycerol tetraether in soils of the Iberian Peninsula, *Biogeosciences*, 11, 2571–2581, doi:10.5194/bg-11-2571-2014, 2014.
- Meriläinen, J., Hynynen, J., Palomäki, A., Reinikainen, P., Teppo, A., and Granberg, K.: Importance of diffuse nutrient loading and lake level changes to the eutrophication of an originally oligotrophic boreal lake: a palaeolimnological diatom and chironomid analysis, *J. Paleolimnol.*, 24, 251–270, 2000.
- Pearson, E. J., Juggins, S., Talbot, H. M., Weckström, J., Rosén, P., Ryves, D. B., Roberts, S. J., and Schmidt, R.: A lacustrine GDGT-temperature calibration from the Scandinavian Arctic to Antarctic: Renewed potential for the application of GDGT-paleothermometry in lakes, *Geochim. Cosmochim. Ac.*, 75, 6225–6238, 2011.
- Peterse, F., Prins, M. A., Beets, C. J., Troelstra, S. R., Zheng, H., Gu, Z., Schouten, S., and Damsté, J. S. S.: Decoupled warming and monsoon precipitation in East Asia over the last deglaciation, *Earth Planet. Sc. Lett.*, 301, 256–264, 2011.
- Peterse, F., van der Meer, J., Schouten, S., Weijers, J. W. H., Fierer, N., Jackson, R. B., Kim, J.-H., and Sinninghe Damsté, J. S.: Revised calibration of the MBT-CBT paleotemperature proxy based on branched tetraether membrane lipids in surface soils, *Geochim. Cosmochim. Ac.*, 96, 215–229, 2012.
- Prahl, F. G., Muehlhausen, L. A., and Zahnle, D. L.: Further evaluation of long-chain alkenones as indicators of paleoceanographic conditions, *Geochim. Cosmochim. Ac.*, 52, 2303–2310, 1988.
- Qiu, J.: The third pole, *Nature*, 454, 393–396, 2008.
- Schouten, S., Hopmans, E. C., and Sinninghe Damsté, J. S.: The organic geochemistry of glycerol dialkyl glycerol tetraether lipids: A review, *Org. Geochem.*, 54, 19–61, 2013.
- Seppä, H. and Birks, H. J. B.: July mean temperature and annual precipitation trends during the Holocene in the Fennoscandian tree-line area: pollen-based climate reconstructions, *Holocene*, 11, 527–539, 2001.
- Shanahan, T. M., Hughen, K. A., and Van Mooy, B. A. S.: Temperature sensitivity of branched and isoprenoid GDGTs in Arctic lakes, *Org. Geochem.*, 64, 119–128, 2013.
- Sinninghe Damsté, J. S., Ossebaar, J., Abbas, B., Schouten, S., and Verschuren, D.: Fluxes and distribution of tetraether lipids in an equatorial African lake: Constraints on the application of the TEX86 palaeothermometer and BIT index in lacustrine settings, *Geochim. Cosmochim. Ac.*, 73, 4232–4249, 2009.
- Sinninghe Damsté, J. S., Rijpstra, W. I. C., Hopmans, E. C., Weijers, J. W. H., Foesel, B. U., Overmann, J., and Dedysh, S. N.: 13,16-Dimethyl Octacosanedioic Acid (iso-Diabolic Acid), a Common Membrane-Spanning Lipid of Acidobacteria Subdivisions 1 and 3, *Appl. Environ. Microb.*, 77, 4147–4154, 2011.
- Sun, Q., Chu, G., Liu, M., Xie, M., Li, S., Ling, Y., Wang, X., Shi, L., Jia, G., and Lü, H.: Distributions and temperature dependence of branched glycerol dialkyl glycerol tetraethers in recent lacustrine sediments from China and Nepal, *J. Geophys. Res.-Biogeo.*, 116, G01008, doi:10.1029/2010jg001365, 2011.
- Thompson, L. G., Yao, T., Davis, M. E., Henderson, K. A., Mosley Thompson, E., Lin, P. N., Beer, J., Synal, H. A., Cole-Dai, J., and Bolzan, J. F.: Tropical climate instability: The last glacial cycle from a Qinghai-Tibetan ice core, *Science*, 276, 1821–1825, 1997.
- Tierney, J. E. and Russell, J. M.: Distributions of branched GDGTs in a tropical lake system: Implications for lacustrine application of the MBT/CBT paleoproxy, *Org. Geochem.*, 40, 1032–1036, 2009.
- van den Wollenberg, A.: Redundancy analysis an alternative for canonical correlation analysis, *Psychometrika*, 42, 207–219, 1977.
- Wang, H., Liu, W., Zhang, C. L., Wang, Z., Wang, J., Liu, Z., and Dong, H.: Distribution of glycerol dialkyl glycerol tetraethers in surface sediments of Lake Qinghai and surrounding soil, *Org. Geochem.*, 47, 78–87, 2012.
- Wang, Y., Kromhout, E., Zhang, C., Xu, Y., Parker, W., Deng, T., and Qiu, Z.: Stable isotopic variations in modern herbivore tooth enamel, plants and water on the Tibetan Plateau: Implications for paleoclimate and paleoelevation reconstructions, *Palaeogeogr. Palaeoclimatol.*, 260, 359–374, 2008.
- Weijers, J. W. H., Schouten, S., Spaargaren, O. C., and Sinninghe Damsté, J. S.: Occurrence and distribution of tetraether membrane lipids in soils: Implications for the use of the TEX86 proxy and the BIT index, *Org. Geochem.*, 37, 1680–1693, 2006.
- Weijers, J. W. H., Schefuss, E., Schouten, S., and Damsté, J. S. S.: Coupled thermal and hydrological evolution of tropical Africa over the last deglaciation, *Science*, 315, 1701–1704, 2007a.
- Weijers, J. W. H., Schouten, S., van den Donker, J. C., Hopmans, E. C., Sinninghe Damsté, J. S.: Environmental controls on bacterial tetraether membrane lipid distribution in soils, *Geochim. Cosmochim. Ac.*, 71, 703–713, 2007b.
- Weijers, J. W. H., Bernhardt, B., Peterse, F., Werne, J. P., Dungait, J. A. J., Schouten, S., and Sinninghe Damsté, J. S.: Absence of seasonal patterns in MBT-CBT indices in mid-latitude soils, *Geochim. Cosmochim. Ac.*, 75, 3179–3190, 2011.
- Wu, X., Dong, H., Zhang, C. L., Liu, X., Hou, W., Zhang, J., and Jiang, H.: Evaluation of glycerol dialkyl glycerol tetraether proxies for reconstruction of the paleo-environment on the Qinghai-Tibetan Plateau, *Org. Geochem.*, 61, 45–56, 2013.
- Wu, W., Ruan, J., Ding, S., Zhao, L., Xu, Y., Yang, H., Ding, W., and Pei, Y.: Source and distribution of glycerol dialkyl glycerol tetraethers along lower Yellow River-estuary-coast transect, *Mar. Chem.*, 158, 17–26, 2014.
- Xie, S., Pancost, R. D., Chen, L., Evershed, R. P., Yang, H., Zhang, K., Huang, J., and Xu, Y.: Microbial lipid records of highly alkaline deposits and enhanced aridity associated with significant uplift of the Tibetan Plateau in the Late Miocene, *Geology*, 40, 291–294, 2012.
- Yang, H., Pancost, R. D., Dang, X., Zhou, X., Evershed, R. P., Xiao, G., Tang, C., Gao, L., Guo, Z., and Xie, S.: Correlations between microbial tetraether lipids and environmental variables in Chinese soils: Optimizing the paleo-reconstructions in semi-arid and arid regions, *Geochim. Cosmochim. Ac.*, 126, 49–69, 2014.

- Yang, H., Lü, X., Ding, W., Lei, Y., Dang, X., and Xie, S.: The 6-methyl branched tetraethers significantly affect the performance of the methylation index (MBT<sup>\*</sup>) in soils from an altitudinal transect at Mount Shennongjia, *Org. Geochem.*, 82, 42–53, 2015.
- Yao, T., Pu, J., Lu, A., Wang, Y., and Yu, W.: Recent Glacial Retreat and Its Impact on Hydrological Processes on the Tibetan Plateau, China, and Surrounding Regions, *Arct. Antarct. Alp. Res.*, 39, 642–650, 2007.
- Yao, T. D., Thompson, L. G., Duan, K. Q., Xu, B. Q., Wang, N. L., Pu, J. C., Tian, L. D., Sun, W. Z., Kang, S. C., and Qin, X. A.: Temperature and methane records over the last 2 ka in Dasuopu ice core, *Sci. China Ser. D*, 45, 1068–1074, 2002.
- Zech, R., Gao, L., Tarozo, R., and Huang, Y.: Branched glycerol dialkyl glycerol tetraethers in Pleistocene loess-paleosol sequences: Three case studies, *Org. Geochem.*, 53, 38–44, 2012.
- Zell, C., Kim, J.-H., Hollander, D., Lorenzoni, L., Baker, P., Silva, C. G., Nittrouer, C., and Sinninghe Damsté, J. S.: Sources and distributions of branched and isoprenoid tetraether lipids on the Amazon shelf and fan: Implications for the use of GDGT-based proxies in marine sediments, *Geochim. Cosmochim. Ac.*, 139, 293–312, 2014.
- Zink, K.-G., Vandergoes, M. J., Mangelsdorf, K., Dieffenbacher-Krall, A. C., and Schwark, L.: Application of bacterial glycerol dialkyl glycerol tetraethers (GDGTs) to develop modern and past temperature estimates from New Zealand lakes, *Org. Geochem.*, 41, 1060–1066, 2010.
- Zink, K. G., Leythaeuser, D., Melkonian, M., and Schwark, L.: Temperature dependency of long-chain alkenone distributions in Recent to fossil limnic sediments and in lake waters, *Geochim. Cosmochim. Ac.*, 65, 253–265, 2001.